Exchange and crystal-field interactions of Ho^{3+} in $GdAl_2$: a single-crystal NMR study

1989 J. Phys.: Condens. Matter 1 10439

(http://iopscience.iop.org/0953-8984/1/51/016)

J. Phys.: Condens. Matter 1 (1989) 10439–10458. Printed in the UK

Exchange and crystal-field interactions of Ho^{3+} in $GdAl_2$: a single-crystal NMR study

D F McMorrow†§, M A H McCausland†, Z-P Han† and J S Abell‡
† The Schuster Laboratory, The University, Manchester M13 9PL, UK
‡ Department of Metallurgy, University of Birmingham, Birmingham B15 2TT, UK

Received 3 July 1989

Abstract. The hyperfine splitting of holmium, as a dilute (1%) substituent in ferromagnetic $GdAl_2$, has been studied by spin-echo NMR at liquid helium temperatures. The measurements were made on oriented single crystals, with fields up to 8 T applied along twofold, threefold and fourfold crystallographic symmetry axes. The field dependence of the hyperfine splitting is interpreted in terms of the standard three-parameter mean-field model for lanthanide ions at sites of cubic symmetry. The crystal-field coefficients are found to be 30% to 40% smaller than those for pure $HoAl_2$; moreover, the molecular field seen by the holmium ion is more than 20% below the lower bound derived from a current model of exchange in RAl_2 compounds. These unexpected results are strikingly confirmed by a recent analysis of FMR data on a dilute Ho : $GdAl_2$ alloy. Possible explanations are considered.

1. Introduction

The RAl_2 cubic Laves phase compounds are singularly well adapted for the study of crystal-field and exchange interactions in rare-earth ferromagnets. They are readily prepared in single-crystal form; moreover, their magnetic properties are satisfactorily described by a simple three-parameter model incorporating the fourth- and sixth-order crystal-field terms appropriate to the cubic symmetry of the lanthanide site and an exchange interaction defined, in the mean-field approximation, by an isotropic molecular-field coefficient (Bak 1974, Purwins *et al* 1974, 1976, Frauenheim and Matz 1979, Kohake *et al* 1982, Eyers *et al* 1982, Schelp *et al* 1983, 1985, 1986, Leson *et al* 1986).

The pure RAl_2 compounds and the isomorphic pseudo-binary alloys $(R, R')Al_2$ have been studied by a variety of techniques including neutron scattering, magnetisation measurements and resonance methods. The work to be described is a NMR study of the field dependence of the hyperfine splitting of Ho^{3+} as a dilute substituent in $GdAl_2$. It is part of a continuing research programme on hyperfine interactions in magnetically ordered RAl_2 compounds (Waind *et al* 1983 (referred to as I), Ross *et al* 1983, Prakash *et al* 1984 (referred to as II), McMorrow *et al* 1986). The principal goals of the project are to ascertain whether or not the three-parameter mean-field (TPMF) model can provide a consistent description of the microscopic and macroscopic properties of the pure

§ Present address: Department of Physics, University of Edinburgh, Mayfield Road, Edinburgh EH9 3JZ, UK.

0953-8984/89/5110439 + 20 $02.50

compounds, and to study the manner in which exchange and crystal-field interactions in mixed alloys depend on the constituents.

The choice of the Ho : $GdAl_2$ system for the present investigation is based partly on the fact that there exists in the literature an unusually good consensus as to the crystal-field coefficients for Ho^{3+} in pure $HoAl_2$ (see II for a summary in 1984) and partly on the advantages of an almost isotropic host with lattice parameters closely matched to those of the pure solute material. The strong molecular field (>20 T) exerted on the holmium ion by its gadolinium neighbours makes it possible to rotate the Ho^{3+} moment into any desired direction by a relatively modest external field. Finally, the dilution of the Ho^{3+} ion in an isotropic host facilitates the observation of NMR by decreasing the nuclear spin–spin interaction and increasing the NMR enhancement factor.

The vast majority of NMR measurements so far reported on rare-earth metals have been carried out on polycrystalline material in zero field. Such measurements are technically straightforward, but interpretation is complicated by domain-wall effects (see, e.g., Barbara and Berthier 1977, Berthier and Devine 1980a, Bowden *et al* 1982, 1983, Barash and Barak 1984, Dressel and Dormann 1988). Such effects can be eliminated by applying a field strong enough to drive out domain walls, but the anisotropy of the hyperfine splitting then causes severe inhomogeneous broadening unless single crystals are used. NMR measurements on metallic single crystals are technically demanding, but are amply rewarded by the detailed information that can be obtained from the anisotropy and field dependence of the hyperfine splitting (Fekete *et al* 1975, Kropp *et al* 1983, Dumelow *et al* 1988).

The measurements to be described were made on single-crystal specimens, with fields up to 8 T along the twofold, threefold and fourfold symmetry axes. A preliminary account of our results for the twofold axis has been given by McMorrow *et al* (1986).

2. Experimental details

The specimens used in this work were obtained from a single crystal of $Ho_{0.01}Gd_{0.99}Al_2$. The crystal was grown by the Czochralski method from a stoichiometric melt in a tungsten crucible in an atmosphere of purified argon (for details see Abell *et al* (1986)). Three rectangular rods, of approximate dimensions 2 mm × 2 mm × 8 mm, were cut from the crystal by spark erosion so that their long axes were parallel to each of the principal crystallographic axes, ⟨001⟩, ⟨011⟩ and ⟨111⟩. The orientation of each rod was determined to better than 1° by Laue x-ray back-scattering. The specimens were lightly etched in dilute hydrochloric acid to remove surface damage.

Each specimen was incorporated as the central conductor in a specially designed coaxial resonator tunable from 5 to 7.5 GHz. Details of the resonator and of the pulsed-microwave spectrometer are given by Carboni *et al* (1989). The resonator was located at the centre of a superconducting solenoid nominally coaxial with the long axis of the crystal and hence with a crystallographic symmetry axis. The estimated maximum deviation of the applied field $\boldsymbol{B}_a$ from the required crystallographic axis is 3°. The measurements were made at liquid helium temperatures, using a conventional spin-echo sequence with pulse durations of 50 to 100 ns.

Since the specimens are non-ellipsoidal, the demagnetising field $\boldsymbol{B}_{dm}$ just inside the metallic surface is non-uniform and, in general, non-collinear with $\boldsymbol{B}_a$. However, the resonator configuration is such that the NMR signals come predominantly from the middle section of the rod. We estimate that the axial and transverse demagnetising factors

on the relevant portions of the specimen surface are respectively -0.08 ± 0.04 and 0.02 ± 0.02. M_s, the saturation magnetisation of $GdAl_2$ at liquid helium temperatures, is 1.07 MA m^{-2} (du Tremolet de Lacheisserie 1988), so the longitudinal and transverse components of the demagnetising field would be respectively $B_{dm\parallel} = -(0.11 \pm 0.05)$ T and $B_{dm\perp} = (0.03 \pm 0.03)$ T if the specimens were uniformly magnetised. Non-uniform magnetisation will marginally reduce these figures. Allowing for the possible sample misalignment mentioned above, we conclude that the *average* deviation of the internal field ($\boldsymbol{B}_a + \boldsymbol{B}_{dm}$) from the required crystallographic axis is at most 4°, with a spread of about 1°, when applied field exceeds 1 T (the lowest field used in our analysis). The effect of angular deviations on the hyperfine parameters is discussed in § 3.5.

3. Theory

Our theoretical model follows that used in I and II. The hyperfine interaction of the ^{165}Ho nucleus ($I = 7/2$) with the electrons of the parent Ho^{3+} ion ($J = 8$) is treated as a perturbation on the electronic ground state; appropriate extra-ionic contributions are included in the effective nuclear Hamiltonian thus obtained (see § 3.3). The ionic energy eigen-states required in the perturbation calculation are obtained by numerical diagonalisation of the 17-dimensional TPMF Hamiltonian for Ho^{3+}. (Only the ground state is significantly populated in the present work, but the excited states contribute to the hyperfine splitting in second order.)

3.1. The electronic Hamiltonian

The interaction of the Ho^{3+} ion with its environment may be expressed, in the mean-field approximation, by the effective TPMF Hamiltonian

$$\mathcal{H}_{el} = \mathcal{H}_{cf} + \mathcal{H}_Z \tag{1}$$

where $\mathcal{H}_{cf}$, the crystal-field term, is specified by the coefficients B_4 and B_6 in the notation of Abragam and Bleaney (1971). As in I and II, we write the Zeeman term in the form

$$\mathcal{H}_Z = -\boldsymbol{\alpha} \cdot \mathbf{J}. \tag{2}$$

In the present context the vector $\boldsymbol{\alpha}$ includes contributions from exchange, from the applied field $\boldsymbol{B}_a$ and from the relatively small dipolar field $\boldsymbol{B}_{dip}$. Thus

$$\boldsymbol{\alpha} = \boldsymbol{\alpha}_{ex} + g\mu_B(\boldsymbol{B}_a + \boldsymbol{B}_{dip}) \tag{3}$$

where g is the Landé factor for Ho^{3+} and μ_B is the Bohr magneton. Since the ion occupies a site of cubic symmetry, the dipolar field is the sum of the Lorentz field $\boldsymbol{B}_L = (\mu_0/3)\boldsymbol{M}_s$ and the demagnetising field $\boldsymbol{B}_{dm}$. Using the data quoted in § 2, we obtain $B_{dip\parallel} = (0.34 \pm 0.05)$ T for the axial component of the dipolar field. The relatively small transverse component does not significantly affect the magnitude of the total field seen by the ion.

Following I (in which $\boldsymbol{B}_a$ was zero and $\boldsymbol{B}_{dip}$ neglected), we express the exchange contribution to $\boldsymbol{\alpha}$ as

$$\boldsymbol{\alpha}_{ex} = (g - 1)\boldsymbol{X} \tag{4}$$

where $\boldsymbol{X}$ is the exchange field acting on the 'projected spin' $\boldsymbol{\sigma} = (g - 1)\boldsymbol{J}$ of the ion

(McCausland and Mackenzie 1979). The exchange field, which will be more fully discussed in § 3.2, is related to the equivalent molecular field $\boldsymbol{B}_m$ notionally acting on the ionic moment $\boldsymbol{\mu} = -g\mu_B\boldsymbol{J}$ by

$$\boldsymbol{B}_m = -(1/g\mu_B)\boldsymbol{\alpha} = -[(g-1)/g\mu_B]\boldsymbol{X}. \tag{5}$$

For Ho^{3+} in $GdAl_2$, $B_m \simeq 20$ T (see § 4.2), so the applied field of up to 8 T can substantially alter the balance between the exchange and crystal-field contributions to $\mathcal{H}_{el}$. In § 4.2 we shall see that the resulting variation in the hyperfine splitting imposes tight constraints on the parameters of the TPMF model.

3.2. The exchange interaction and the mean-field approximation

The nature of the exchange interaction between rare-earth ions in metals has been much discussed in the past two decades. It is universally agreed that the interaction is mediated by conduction electrons, but now widely recognised that it is not adequately described by the so called RKKY model in the simple form developed by de Gennes (1962). Campbell (1972) has cogently argued that the dominant mechanism, at least in magnetically concentrated systems, is f–d exchange rather than the f–s exchange posited in the standard RKKY model (see, e.g., Taylor 1971). The dominance of the 4f–5d interaction in RAl_2 and other intermetallic compounds has been corroborated by Zipper *et al* (1984) and by Belorizky *et al* (1987, 1988a, b).

Orbital and multipolar contributions to the inter-ionic interaction have also been invoked to explain particular aspects of the behaviour of rare-earth intermetallics (Levy 1969, Dunlap *et al* 1973, Schmitt *et al* 1977, Barbara *et al* 1977, 1983, Aleonard *et al* 1988, Morin and Schmitt 1988). Anisotropic interactions are undoubtedly important in some equiatomic compounds but their effects in RAl_2 compounds appear to be marginal. Studies of magnetic excitations by neutron inelastic scattering show that, even in compounds such as $DyAl_2$ and $HoAl_2$ with strong single-ion anisotropy, the inter-ionic interaction is dominated by isotropic Heisenberg exchange (Holden *et al* 1984, Schelp *et al* 1983, 1985). *A fortiori*, we may take it that anisotropic exchange plays a negligible part in the Gd-rich alloy under discussion.

Anticipating the discussion in § 4 we now set out, as explicitly as possible, some assumptions often tacitly made in discussions of exchange in rare-earth metals. For the reasons outlined above, we restrict our attention to indirect Heisenberg exchange. We also follow de Gennes (1962) in using the operator $(g-1)\boldsymbol{J}$, here denoted by $\boldsymbol{\sigma}$, as the effective ionic spin entering the exchange interaction. The validity of that procedure does not depend on the particular assumptions made by de Gennes about the nature of the conduction electrons; it is a simple consequence of the fact that J remains a good quantum number for heavy rare-earth ions in solids.

3.2.1. Pure compounds. Irrespective of the precise character of the conduction band, the interaction between two rare-earth ions in a *pure* compound will have the general form

$$\mathcal{H}_{ij} = -\mathcal{A}^2 f(\boldsymbol{r}_{ij})\boldsymbol{\sigma}_i \cdot \boldsymbol{\sigma}_j \tag{6}$$

where $\mathcal{A}$ is a measure of the strength of the coupling between the spin on each ion and the conduction electrons and $f(\boldsymbol{r})$ describes the spatial variation of the conduction-electron polarisation. If the response of the conduction electrons is linear, so that the conduction-electron polarisation due to several ions is additive, then, in the mean-field

approximation ($\boldsymbol{\sigma}_j \rightarrow \langle\boldsymbol{\sigma}\rangle$), the 'exchange field' acting on a representative ionic spin $\boldsymbol{\sigma}_i$ is

$$\boldsymbol{X} = \mathcal{J}_0\langle\boldsymbol{\sigma}\rangle \tag{7}$$

where

$$\mathcal{J}_0 = \mathcal{A}^2 \sum_j f(\boldsymbol{r}_{ij}). \tag{8}$$

The exchange coefficient $\mathcal{J}_0$ is related to the parameters $J(q)$ and $J'(q)$ commonly used in the analysis of magnetic excitations (see, e.g., Schelp *et al* 1985) by

$$\mathcal{J}_0 = 2[J(0) + J'(0)]/(g-1)^2. \tag{9}$$

It is also related to the conventional molecular-field constant λ, defined by $\boldsymbol{B}_m = \lambda\langle\boldsymbol{\mu}\rangle$, by

$$\mathcal{J}_0 = [g\mu_B/(g-1)]^2\lambda. \tag{10}$$

In the absence of crystal-field effects the Curie temperature T_C and the paramagnetic Weiss constant θ are given, in the mean-field approximation, by

$$T_C = \theta = (g\mu_B)^2 J(J+1)\lambda/(3k) = G\mathcal{J}_0/(3k) \tag{11}$$

where $G = (g-1)^2 J(J+1)$ is the de Gennes factor. If crystal-field effects are in fact negligible, *and* if $\mathcal{J}_0$ is constant across a given alloy series, we at once obtain a linear relationship between T_C and G, the so called de Gennes relationship. If, on the other hand, crystal-field effects are significant, equation (11) should be replaced by the implicit equation

$$\lambda\chi_0(T_C) = 1 \tag{12}$$

where $\chi_0(T)$ is the crystal-field-only susceptibility per ion (see, e.g., Leson *et al* 1986). Thus, given the crystal-field coefficients, one can in principle derive λ, hence $\mathcal{J}_0$, from the measured Curie temperature. It should be remembered, however, that mean-field theory tends to overestimate the magnetic ordering temperature for a given exchange coupling (see Rushbrooke and Wood 1958, Smart 1966). Consequently, the true value of $\mathcal{J}_0$ is likely to exceed that derived from measured Curie temperatures using equations (11) or (12).

Several authors have noted systematic variations of $\mathcal{J}_0$ across the RAl_2 and other intermetallic alloy series (Waind *et al* 1983, Schelp *et al* 1985, Belorizky *et al* 1987, 1988a). In general, $\mathcal{J}_0$ decreases monotonically with increasing atomic number. By comparing data on R–R interactions in alloys with non-magnetic partners (RAl_2, RZn, RNi_5) with R–M interactions in alloys with magnetic (M) partners (RCo_2, $R_2Fe_{14}B$), Belorizky *et al* (1988a) have argued that the variation in the inter-ionic coupling is associated principally with the coupling between the lanthanide ion and 5d conduction electrons. This implies, in the language of the present paper, that the decrease of $\mathcal{J}_0$ across the RAl_2 series is due to a variation in the coupling coefficient $\mathcal{A}$ and not to a change in the function $f(\boldsymbol{r})$. The same conclusion follows from the work of Belorizky *et al* (1987), where the variation of $\mathcal{A}$ across R–Fe and R–Co compounds is attributed to the decrease of the radius of the 4f shell with increasing atomic number.

3.2.2. Mixed alloys. The foregoing discussion indicates that the appropriate generalisation of equation (6) to an alloy containing more than one rare-earth species is

$$\mathcal{H}_{ij} = \mathcal{A}(R_i)\mathcal{A}(R_j)f(\boldsymbol{r}_{ij})\boldsymbol{\sigma}_i \cdot \boldsymbol{\sigma}_j \tag{13}$$

where $\mathcal{A}(R)$ denotes the strength of the coupling between the spin on an ion of species R and the conduction electrons. Assuming additivity as before, the exchange field seen by an ion of species R is

$$\boldsymbol{X} = \mathcal{A}(R) \sum \mathcal{A}(R_j) f(\boldsymbol{r}_{ij}) \langle \boldsymbol{\sigma}_j \rangle. \tag{14}$$

In general, $\boldsymbol{X}$ will vary from one R ion to another because of the random distribution of species over neighbouring sites†. In the special case of a *dilute* solution of R in $R'Al_2$, all $\mathcal{A}(R_j)\langle \boldsymbol{\sigma}_j \rangle$ in the right-hand side of equation (14) may to a good approximation be replaced by $\mathcal{A}(R')\langle \boldsymbol{\sigma}' \rangle$. The equation then simplifies to

$$\boldsymbol{X} = \mathcal{J}_0(R:R')\langle \boldsymbol{\sigma}' \rangle \tag{15}$$

where $\mathcal{J}_0(R:R')$, the effective exchange constant for R in $R'Al_2$, is given by

$$\mathcal{J}_0(R:R') = \mathcal{A}(R)\mathcal{A}(R') \sum_j f(\boldsymbol{r}_{ij}). \tag{16}$$

It follows from equation (8) that

$$\mathcal{J}_0(R:R') = \{\mathcal{J}_0(R)\mathcal{J}_0(R')\}^{1/2} \tag{17}$$

where $\mathcal{J}_0(R)$ and $\mathcal{J}_0(R')$ are respectively the exchange coefficients for pure RAl_2 and $R'Al_2$. Another consequence of the model under discussion is that

$$\mathcal{J}_0(R':R) = \mathcal{J}_0(R:R'). \tag{18}$$

The expressions obtained above will be critically re-examined in § 4.3.

3.3. The hyperfine interaction

The theory of the hyperfine splitting in rare-earth solids has been described in detail elsewhere (McCausland and Mackenzie 1979, I, II) and will not be rehearsed here. It will suffice to recall that the hyperfine interaction in the solid may be described by an effective Hamiltonian of the form

$$\mathcal{H} = h\{a_t I_z + P_t(I_z^2 - \tfrac{1}{3}\boldsymbol{I}^2) + wI_z^3\} \tag{19}$$

where $\boldsymbol{I}$ is the nuclear spin and the z axis is parallel to $\langle \boldsymbol{J} \rangle$. The dominant intra-ionic contributions to a_t and P_t and the wholly intra-ionic pseudo-octupolar term w are calculated by treating the free-ion hyperfine interaction as a perturbation, carried to second order, on the electronic Hamiltonian $\mathcal{H}_{el}$. The accuracy of the perturbation calculation has been checked by numerical diagonalisation of the 136-dimensional Hamiltonian for the combined electronic–nuclear system (see Carboni *et al* 1988) and found to be adequate.

† If $f(\boldsymbol{r}_{ij})$ varies slowly over regions containing many spins we may average over j in equation (14). Then

$$\boldsymbol{X} \simeq \mathcal{A}(R)\overline{\mathcal{A}\langle \boldsymbol{\sigma} \rangle} \sum_j f(\boldsymbol{r}_{ij})$$

where the bar denotes an average over alloy composition. This, with equation (8), is the basis of equation (7) in I which, subject to the qualification just mentioned, is the generalisation of equation (15) to alloys of arbitrary composition.

By far the largest contribution to the hyperfine splitting is the first-order intra-ionic dipolar term

$$A\langle \boldsymbol{J} \rangle \cdot \boldsymbol{I} = A\langle J_z \rangle I_z \tag{20}$$

where A is the free-ion dipole coupling coefficient. Next in importance comes the first-order intra-ionic quadrupole term

$$C\langle 3J_z^2 - \boldsymbol{J}^2 \rangle (I_z^2 - \tfrac{1}{3}\boldsymbol{I}^2) \tag{21}$$

where $C = P_0'/[J(2J-1)]$ is the free-ion quadrupole coupling coefficient in the notation of Bunbury *et al* (1989). The second-order contributions to a_t and P_t are dominated by terms in A^2, while the octupolar term, which causes a small but measurable asymmetry in the quadrupole-split NMR spectrum, is proportional to AC (see Bunbury *et al* 1989). Extra-ionic contributions to the hyperfine splitting are discussed below.

3.3.1. Extra-ionic dipolar terms. As in II, we write the extra-ionic hyperfine field (HFF) in the form

$$\boldsymbol{B}'' = \boldsymbol{B}_a + \boldsymbol{B}_{dip} + \boldsymbol{B}_{ce} + \boldsymbol{B}_{orb} \tag{22}$$

where

$$\boldsymbol{B}_{ce} = K_p \langle \boldsymbol{\sigma}_p \rangle + K_n \bar{\boldsymbol{\sigma}} \tag{23}$$

and

$$\boldsymbol{B}_{orb} = K_{orb}(2-g)\langle \boldsymbol{J} \rangle \tag{24}$$

respectively denote the contributions of spin- and orbitally-polarised conduction electrons. In the present context, $\boldsymbol{\sigma}_p = (g-1)\boldsymbol{J}$ and $\bar{\boldsymbol{\sigma}} \simeq \langle \boldsymbol{\sigma}' \rangle = (g'-1)\langle \boldsymbol{J}' \rangle$ are the projected spins of the Ho^{3+} probe ions and of the Gd^{3+} host ions, respectively.

Since the extra-ionic field is small compared with the intra-ionic field and our NMR measurements were made with the applied field close to crystallographic symmetry axes, we may with negligible error assume that all contributions to $\boldsymbol{B}''$ are collinear with $\langle \boldsymbol{J} \rangle$ and hence with the much larger intra-ionic hyperfine field $\boldsymbol{B}'$. (Any data points for which that is not a good approximation have been rejected from the analysis described in § 4.2. The effects of angular deviations on the hyperfine parameters are discussed in § 3.5.) We may therefore express a_t as the algebraic sum of the intra-ionic term $a' \simeq A\langle J_z \rangle$ and an extra-ionic term

$$a'' = (\mu_N/hI)B'' \tag{25}$$

where μ_N is the nuclear moment of ^{165}Ho ($I = 7/2$) and

$$B'' = B_a + B_{dip} - K_n\langle \sigma' \rangle - [(g-1)K_p + (2-g)K_{orb}]\langle J_z \rangle. \tag{26}$$

The negative signs before the factors K reflect the fact that hyperfine fields are reckoned positive when parallel to the ionic moment $\langle \boldsymbol{\mu} \rangle$ and hence antiparallel to $\langle \boldsymbol{J} \rangle$.

3.3.2. Extra-ionic quadrupolar terms. The nominally cubic symmetry of the lanthanide site in RAl_2 compounds can be broken by several mechanisms, resulting in a non-vanishing extra-ionic contribution to the quadrupole splitting (see McCausland and Mackenzie 1979, Dormann *et al* 1984, Belorizky *et al* 1984, Belorizky and Berthier 1986, Dressel *et al* 1988). The contributions of all such mechanisms to the electric field gradient

in the system under discussion are believed to be insignificant with the possible exception of orbital polarisation of d-character conduction electrons. In general, the orbital polarisation depends in a complicated manner on the electric multipole moments of the parent ion (Belorizky *et al* 1984, Belorizky 1989). Since, however, the contribution of orbital polarisation to the total electric field gradient seen by the nucleus in RAl_2 compounds is less than 1% and, to a first approximation, varies as $\langle 3J_z^2 - \boldsymbol{J}^2 \rangle$ (Belorizky *et al* 1984), it may without serious error be represented as a small change in the intra-ionic coupling coefficient C in expression (21).

3.4. Numerical considerations

In order to calculate the field dependence of the hyperfine splitting *ab initio*, we need to assign numerical values to the three parameters of the TPMF model (B_4, B_6 and $\mathcal{J}_0$(Ho : Gd)) and to the several constants relating directly to the hyperfine interaction. Among the latter, we take $A = (812 \pm 1)$ MHz and $C = (0.52 \pm 0.03)$ MHz (after Bleaney 1972); also $\mu_N = (4.05 \pm 0.05)$ nuclear magneton (Haberstroh *et al* 1972), whence $a''/B'' = (8.9 \pm 0.1)\ \text{MHz T}^{-1}$.

Not all of the extra-ionic contributions enter the calculation in an independent manner. For example, the extra-ionic quadrupole interaction can be included with the first-order intra-ionic term by replacing C by C_{eff} in the expression (21) (see § 3.3.2). Previous NMR studies of Ho^{3+} in RAl_2 compounds (I, II) indicate that $C_{\text{eff}} \simeq 0.51$ MHz, which is within the uncertainty on the value of C quoted above. Similarly, we may collect together those terms in the dipolar interaction that involve $\langle J_z \rangle$, and define an effective coupling coefficient

$$A_{\text{eff}} = A + A'' \tag{27}$$

where

$$A'' = -(\mu_N/hI)[(g-1)K_p + (2-g)K_{\text{orb}}] \tag{28}$$

represents the extra-ionic terms induced by the parent ion (see equations (20), (25) and (26)). Finally, we observe that $B_{\text{dip}} - K_n\sigma'$ forms a single field-independent contribution to the total hyperfine field; we shall denote the corresponding contribution to a_t by $a''_{\text{host}} = (\mu_n/hI)(B_{\text{dip}} - K_n\langle\sigma'\rangle)$. Previous estimates of the factors K give $K_p \simeq -5.7$ T, $K_n \simeq 0.8$ T and $K_{\text{orb}} \simeq 0.25$ T (I, II). Setting $B_{\text{dip}} \simeq 0.34$ T, we obtain $a''_{\text{host}} \simeq -23$ MHz and $A'' \simeq 11$ MHz, whence $A_{\text{eff}} \simeq 823$ MHz. (We have taken $g' = 1.992$ for Gd^{3+} (Abragam and Bleaney 1971), whence $\langle\sigma'\rangle = 3.472$.)

It will now be clear that all extra-ionic contributions to the hyperfine splitting are rather small (<1%). The field dependence of the splitting is therefore determined principally by the state of the parent ion and hence by the exchange and crystal-field coefficients implicit in equation (1). Our *a priori* estimates of these quantities, given in the top row of table 1, are obtained as follows. Since the lattice parameters of $GdAl_2$ and $HoAl_2$ differ by only 1%, it is reasonable to suppose that the crystal-field coefficients for Ho^{3+} in $GdAl_2$ will be close to those for the pure compound. We have therefore adopted weighted means of published values of B_4 and B_6 for pure $HoAl_2$ (see II). For $\mathcal{J}_0$(Ho : Gd) we use equation (17), which in turn requires numerical estimates for $\mathcal{J}_0$(Gd) and $\mathcal{J}_0$(Ho).

We have already noted the tendency of mean-field theory to underestimate $\mathcal{J}_0$ for a given value of T_c. On the other hand, du Tremolet de Lacheisserie (1988) finds that the critical exponents for $GdAl_2$ are closer to the mean-field than to the Heisenberg values

Table 1. Exchange and crystal-field coefficients and hyperfine parameters for Ho^{3+} in $GdAl_2$.

	$\mathcal{J}_0(\mathrm{Ho:Gd})/k$ (K)	$10^4 B_4/k$ (K)	$10^6 B_6/k$ (K)	a''_{host} (MHz)	A_{eff} (MHz)	C_{eff} (MHz)
A priori[a]	30 ± 3	−8.7 ± 0.3	7.7 ± 0.3	−23	823	0.51
NMR[b]	20.9 ± 0.6	−6.1 ± 0.2	4.6 ± 0.2	−23	825.8 ± 0.3	0.500 ± 0.002
FMR[c]	19.2 ± 1.1	−6.3 ± 0.4	4.4 ± 0.3	—		
Mean[d]	20.5 ± 0.5	−6.1 ± 0.2	4.5 ± 0.2	—		

[a] See § 3.4.
[b] Present work. All parameters free except a''_{host}: see § 4.2.
[c] After Teale *et al* (1989).
[d] Weighted mean of NMR and FMR results.

(a result attributed to the long-range nature of the exchange interaction). It may not, therefore, be unreasonable to assume that the exchange coefficient for $GdAl_2$ lies between the values derived from T_C and from θ. Setting $T_C = 168.3$ K and $\theta = 189$ K (du Tremolet de Lacheisserie 1988) and $G = 15.50$ in equation (11), we thus obtain $\mathcal{J}_0(\mathrm{Gd})/k = (35 \pm 2)$ K.

The relationship between $\mathcal{J}_0$ and T_C (or θ) for $HoAl_2$ is complicated by the crystal-field interaction; moreover, published values of T_C range from 27 K (Harris *et al* 1965) to 33 K (Barbara *et al* 1975; these authors also give $\theta = 36$ K). Schelp *et al* (1983, 1985), using equation (12) with $T_C = 31.5$ K and crystal-field parameters obtained by fitting magnetisation measurements over a wide range of temperatures, obtain a molecular-field constant λ which corresponds to $\mathcal{J}_0/k = 22$ K. This figure agrees well with that deduced from their low-temperatures measurements of $J(0)$ and $J'(0)$ (equation (9)), which suggests that the mean-field relationship (12) is not seriously in error. Rhyne and Koon (1983), also using neutron inelastic scattering at low temperatures, obtain a value of $J(0) + J'(0)$ close to that of Schelp *et al*, albeit with somewhat different crystal-field parameters. On the other hand, Prakash *et al* (1984), using a weighted mean of all available crystal-field parameters for $HoAl_2$, obtain $\mathcal{J}_0/k = (27 \pm 1)$ K from low-temperature measurements of the hyperfine splitting. They attribute the discrepancy between this and earlier estimates based wholly or partly on T_C to the defects of mean-field theory in the neighbourhood of the ordering transition. Both values of $\mathcal{J}_0$ mentioned above were calculated using the commonly accepted g value of 5/4, which corresponds to pure Russell–Saunders coupling; allowance for intermediate coupling, which gives $g = 1.242$ (Rajnak and Krupke 1967, Crosswhite *et al* 1977), will increase them by $\simeq 7\%$. Taking into account all the available data, we conclude that $\mathcal{J}_0(\mathrm{Ho})/k = (26 \pm 3)$ K.

Substitution of the figures obtained above into equation (17) gives

$$27\ \mathrm{K} < \mathcal{J}_0(\mathrm{Ho:Gd})/k < 33\ \mathrm{K}. \tag{29}$$

It must be emphasised that whereas the upper limit ($\simeq$33 K) is somewhat uncertain, the tendency of mean-field theory to underestimate $\mathcal{J}_0$ for a given T_C means that the figure of 27 K must be regarded as a definite lower bound for the effective exchange coefficient in the context of the model described above. The value of α_{ex} entering the TPMF Hamiltonian (equations (1) to (3)) follows from equations (4) and (15); setting $g = 1.242$ and $\sigma' = 3.472$ we obtain $\alpha_{\mathrm{ex}} = 0.840\mathcal{J}_0(\mathrm{Ho:Gd})$.

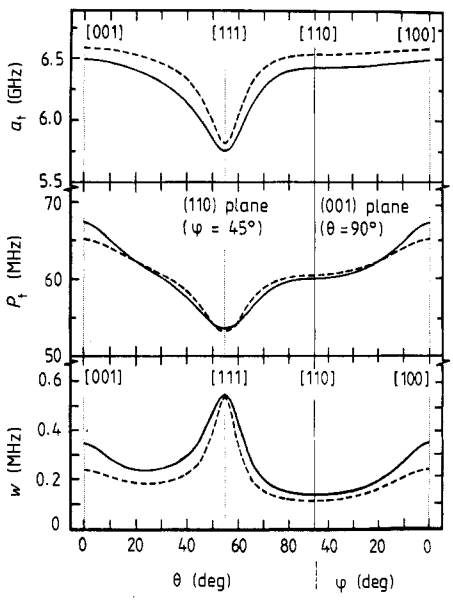

Figure 1. Calculated variation of the dipolar, quadrupolar and octupolar hyperfine parameters of Ho^{3+} in $GdAl_2$ at $T = 0$ as the applied field $\boldsymbol{B}_a$ is rotated in the (110) and (001) planes. The full and broken curves are for $B_a = 1$ T and $B_a = 8$ T respectively. θ and φ are spherical coordinates with respect to the crystallographic axes $\boldsymbol{a} = [100]$, $\boldsymbol{b} = [010]$, $\boldsymbol{c} = [001]$.

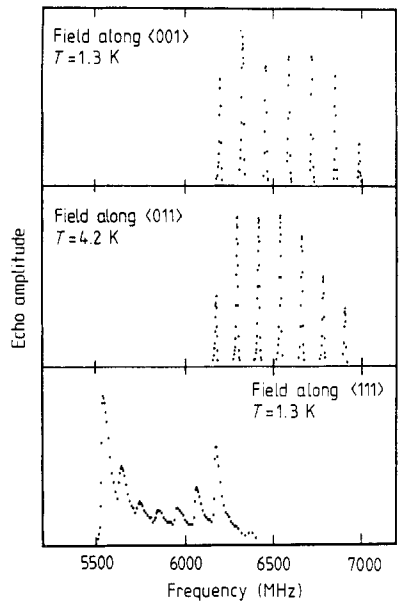

Figure 2. Spin-echo spectra of ^{165}Ho in $GdAl_2$ with a field of 8 T applied along the fourfold, twofold and threefold symmetry axes. The units of the vertical axis are arbitrary.

3.5. Angular effects

If the field is applied in an arbitrary direction relative to the crystallographic axes, the gadolinium and holmium moments will not in general be collinear with each other or with $\boldsymbol{B}_a$. In order to diagonalise $\mathcal{H}_{el}$ we need to find the magnitude and direction of $\boldsymbol{\alpha}$ (equation (3)) as a function of $\boldsymbol{B}_a$. This has been done by an iterative procedure described in the appendix. The exchange and crystal-field coefficients used in the calculation are those given in the second row of table 1.

The calculated variations of the dipolar, quadrupolar and octupolar hyperfine parameters as the applied field is rotated in the (110) and (001) planes are shown in figure 1. It will be seen that the parameters are insensitive to small angular deviations of the field from the twofold and fourfold axes, but vary rapidly in the neighbourhood of the threefold axis. The maximum deviation of the internal field due to sample misalignment and to the non-uniform demagnetising field is estimated to be 4° (see § 2). The worst-case systematic error on the measured NMR frequency due to a 4° deviation is only 6 MHz (0.1%) when the applied field is nominally along a ⟨001⟩ or ⟨011⟩ axis, but is over 150 MHz (2.5%) when the field is nominally along a ⟨111⟩ axis.

Besides the systematic errors discussed above, there exists a spatial inhomogeneity of hyperfine parameters associated with the non-uniformity of the internal field. This inhomogeneity is dominated by angular effects, so the concomitant broadening of the NMR lines will be most marked when the applied field is close to the ⟨111⟩ direction.

4. Results and discussion

4.1. General observations

Representative NMR spectra are shown in figure 2. All spectra have been fitted to a nuclear spin Hamiltonian of the form (19). The resulting values of a_t, P_t and w are plotted against the applied field in figure 3.

4.1.1. Field along ⟨001⟩. It was not possible to detect NMR signals at 4.2 K when fields greater than 0.2 T were applied along the ⟨001⟩ direction, but satisfactory spectra were obtained when the temperature was reduced to 1.3 K.

The anomalously low values of a_t obtained at and below 1 T suggest that the magnetisation is rotating towards the easier ⟨011⟩ direction in low fields. This is compatible with our observation of substantially increased enhancement of the NMR signal at low fields. The hyperfine parameters measured at and below 1 T have therefore been omitted from the analysis described in § 4.2.

As noted in I, the small electronic energy gap associated with the ⟨001⟩ direction gives rise to large second-order effects. These are most clearly evident in the behaviour of the quadrupole parameter P_t (figure 3(*a*)). The field-induced increase in $\langle J_z^2 \rangle$ and hence in the first-order quadrupole splitting (equation (21)) is actually outweighed by the faster decrease in the second-order term as the electronic energy gap increases (see figure 4 in I). The small energy gap is also believed to be responsible for the difficulty in detecting NMR at 4.2 K.

4.1.2. Field along ⟨001⟩. The strongest NMR signals were obtained with the applied field $\boldsymbol{B}_a$ along ⟨011⟩, the easy direction direction of magnetisation for Ho^{3+} on $GdAl_2$. Sharp seven-line spectra were obtained at 4.2 K; no shift in the hyperfine splitting was detected when the temperature was reduced to 1.3 K.

The microwave power required to maximise the echo signals at the lowest fields was two orders of magnitude lower than that at fields above 1 T. This suggests that the zero-field spectrum comes from domain walls, a conclusion at variance with that of Waind *et al* (I). On the other hand, the value of a_t obtained by extrapolating our data to zero field is approximately 6410 MHz, very close to the zero-field value of (6415 ± 2) MHz obtained by Waind *et al* in polycrystalline Ho:$GdAl_2$. The difference is much smaller than that which would be expected for spins oriented along ⟨001⟩ axes or, for that matter, along the very hard ⟨111⟩ direction (see I for details). We infer that the zero-field signals reported in I originated in the wings of domain walls, where the orientation of the holmium moments approximates to the easy ⟨011⟩ direction.

4.1.3. Field along ⟨111⟩. The marked reduced dipolar and quadrupolar splittings (figures 2 and 3(*c*)) reflect the strong quenching of the holmium moment along the hard ⟨111⟩ direction. The spectra suffer from severe inhomogeneous broadening, particularly in low fields. This is readily understood in terms of the small angular variations in the local field (§ 2), together with the marked angular sensitivity of the hyperfine parameters in the neighbourhood of the threefold symmetry axis (figure 1). The broadening is already apparent at 8 T (figure 2); below 4 T the quadrupole splitting was unresolved. We therefore display only the high-field hyperfine parameters in figure 3(*c*).

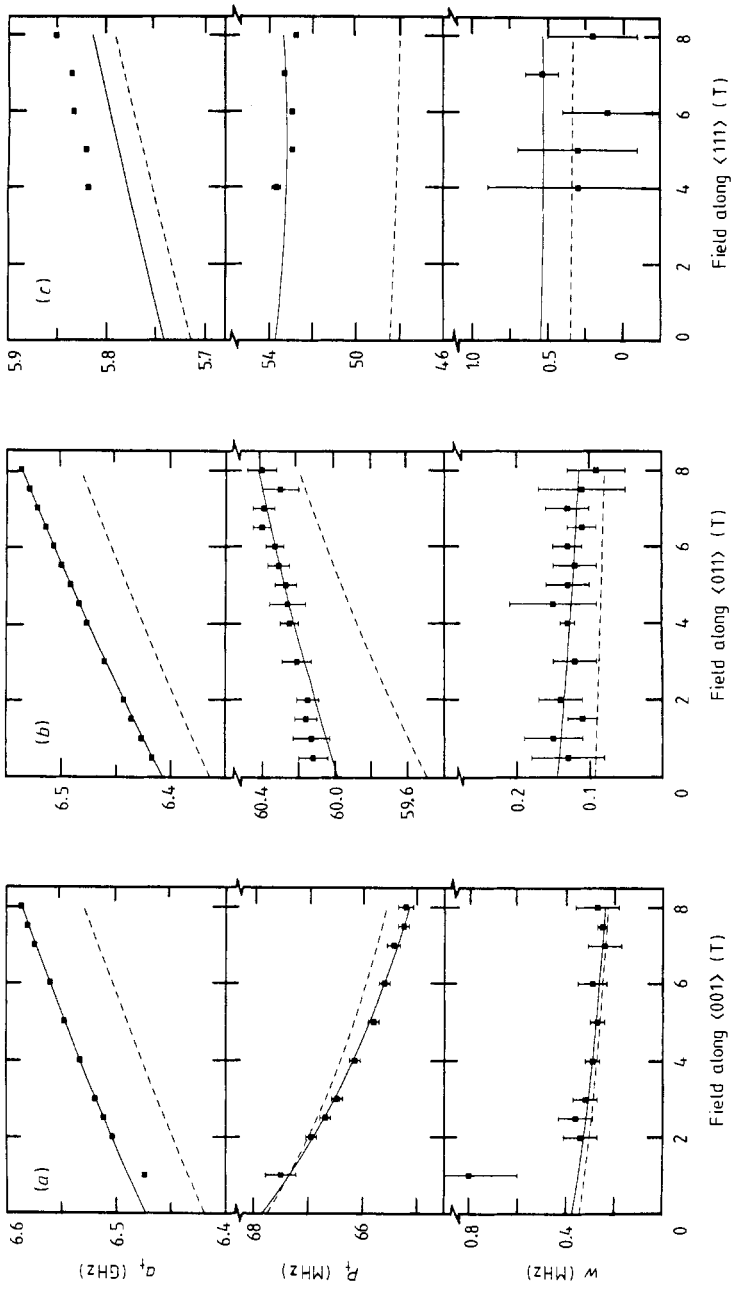

Figure 3. Calculated and measured field dependence of the dipolar, quadrupolar and octupolar hyperfine parameters of Ho^{3+} in $GdAl_2$ at liquid helium temperatures: (*a*) applied field $\boldsymbol{B}_a$ along a ⟨001⟩ axis; (*b*) $\boldsymbol{B}_a$ along a ⟨011⟩ axis; (*c*) $\boldsymbol{B}_a$ along a ⟨111⟩ axis. Error bars are omitted from the experimental points for a_t because the uncertainties are smaller than the size of the squares. The broken curves have been calculated from the *a priori* parameters given in the top row of table 1. The full curves represent the least-squares fit to the ⟨001⟩ and ⟨011⟩ data; the parameters of the fit are given in the second row in table 1. See text for a discussion of the ⟨111⟩ data.

Table 2. Correlation matrix for the exchange and crystal-field coefficients and for the hyperfine parameters derived from a least-squares fit to the NMR data.

	$\mathcal{J}_0$	B_4	B_6	A_{eff}	C_{eff}
$\mathcal{J}_0$	1.000				
B_4	−0.974	1.000			
B_6	0.985	−0.990	1.000		
A_{eff}	0.880	−0.949	0.946	1.000	
C_{eff}	0.946	−0.981	0.976	0.907	1.000

4.2. Analysis in terms of the TPMF model

As explained in § 3.5, the NMR data for the ⟨111⟩ direction are subject to significant systematic errors due to possible misalignment. Expect where stated otherwise, the analysis which follows is restricted to the ⟨001⟩ and ⟨011⟩ directions. For the reason given in § 4.1.1 we also discount the ⟨001⟩ data for $B_a \leqslant 1$ T.

It is clear from figure 3 that the *a priori* parameters, given in the top row of table 1, give a poor description of the ⟨001⟩ and ⟨011⟩ data. Moreover, the differences between calculated and measured hyperfine parameters for the ⟨111⟩ direction cannot consistently be explained in terms of a misalignment of the crystal: the discrepancy for the dipolar splitting parameter implies a misalignment of 3°, whereas that for the quadrupolar splitting implies a misalignment of over 10° which, in any case, is much greater than the estimated upper bound given in § 2.

Some improvement can be obtained by adjusting one or more of the ancillary parameters a''_{host}, A_{eff} and C_{eff}, but the required values of the extra-ionic terms are implausibly large and even then the fit remains unsatisfactory. We conclude that the measured hyperfine splitting cannot be reconciled with the TPMF model so long as we adhere to the *a priori* exchange and crystal-field coefficients.

A much better fit is obtained if the exchange and crystal-field parameters are treated as free parameters, leaving a''_{host}, A_{eff} and C_{eff} at their *a priori* values. However, the residual discrepancies indicate that readjustment of some or all of the extra-ionic terms is justified. In principle, the constant term a''_{host} can be distinguished from A_{eff} by the fact that the contribution of the latter to a_t varies with $\langle J_z \rangle$. In practice, it is not possible to extract both terms from our experimental data because the total variation in $\langle J_z \rangle$ is only 2.5% when the ⟨111⟩ data are excluded. We are therefore obliged to fix either A_{eff} or a''_{host}. The value of K_n on which a''_{host} is based is believed to be more reliable than the values of K_p and K_{orb} underlying the extra-ionic contributions to A'', and we have therefore assigned a''_{host} its *a priori* value. The results of a least-squares fit in which the remaining five parameters are free are given in the second row of table 1. The quality of the fit, indicated by the full curves in figures 3(*a*) and 3(*b*), is excellent; the reduced value of χ^2 is 0.2. It should be noted, however, that the parameters of the fit are strongly correlated: see table 2.

It is not surprising that a better fit is obtained with five free parameters than with three. However, it should be remembered that the extra-ionic terms are small and therefore give little real room for manoeuvre. The fact that the fitted values of A_{eff} and C_{eff} are very close to the *a priori* figures gives us considerable confidence in the validity of the fit. Moreover, *all* of the ⟨111⟩ data (which, as explained above, were not included in the fit) are consistent with the fitted parameters if we assume an angular deviation of

about 2.5° between the internal field and the ⟨111⟩ axis. This is well within the expected limit of 4° (§ 2).

The most striking confirmation of the fitted TPMF parameters, however, comes from an independent FMR study of single crystals of $GdAl_2$ containing 0.2% Ho as a substitutional impurity. The temperature dependence of the anisotropy fields along the ⟨100⟩ and ⟨111⟩ directions, determined from the FMR data, has been analysed in terms of the TPMF model by Teale *et al* (1989). The resulting exchange and crystal-field coefficients, given in the third row of table 1, are in close agreement with those derived from our NMR measurements.

The FMR work is complementary to ours in two respects. First, it includes data for the ⟨111⟩ direction which, as explained above, were excluded from our analysis; conversely, the NMR results include the ⟨011⟩ direction which, for technical reasons, was excluded from the analysis of Teale *et al* (1989). Second, the two sets of data reflect distinct features of the holmium ion: the hyperfine splitting depends principally on the nature of the ionic ground state, whereas the anisotropy field depends on the angular dependence of the free energy and hence of the thermally populated energy levels. The close agreement between the exchange and crystal-field coefficients derived from the NMR and FMR data therefore lend strong support for the TPMF model.

One common feature of the NMR and FMR measurements is that they probe the material only to a depth of the order of the microwave penetration depth. It might therefore be argued that the resulting exchange and crystal-field coefficients are uncharacteristic of the bulk material. However, any significant variation of the TPMF parameters within the skin depth (estimated to be at least 1000 lattice spacings at the relevant frequencies) would be manifested by severe inhomogeneous broadening of the NMR spectra. No such broadening is observed, except for the ⟨111⟩ spectra, for which an alternative explanation has been given in § 4.1.3. We do not, of course, exclude the possibility of true surface effects within the few outermost atomic layers. Such effects, being restricted to a small fraction of the skin depth, would not contribute appreciably to the observed spectra. We conclude that our results cannot be dismissed as a surface effect.

In the fourth row of of table 1 we give the weighted mean of the TPMF parameters derived from the NMR and FMR measurements. The values of X, α_{ex} and B_m corresponding to the mean value of $\mathcal{J}_0$(Ho:Gd) are respectively $X/k = (71 \pm 2)$ K, $\alpha_{ex}/k = (17.2 \pm 0.5)$ K and $B_m = (20.7 \pm 0.6)$ T. These results follow from equations (4), (5) and (15).

4.3. Discussion

The available evidence indicates that the TPMF model accurately describes the behaviour of Ho^{3+} in $GdAl_2$. In particular, the fact that the data for all three principal crystallographic directions are well described by a single set of parameters confirms that the exchange interaction of the solute ions with the host medium is isotropic. On the other hand, it appears that the exchange and crystal-field parameters for a dilute $R:R'Al_2$ system are not as simply related to those for the terminal compounds as we supposed.

We first consider the crystal-field coefficients. The values of B_4 and B_6 derived from the NMR and FMR measurements are respectively 30% and 40% smaller than those for pure $HoAl_2$. These differences are too large to be attributed to the marginally larger lattice constant of the $GdAl_2$ host. If B_4 and B_6 vary as a^{-5} and a^{-7} respectively (see e.g., Purwins *et al* 1974), the NMR and FMR results might in principle be explained by a 5%

isotopic expansion of the host lattice in the neighbourhood of each solute ion. Since the ionic radius of holmium is 5% *smaller* than that of gadolinium, such an expansion is highly improbable. The only remaining possibility is that the conduction–electron contribution to the crystal field in $GdAl_2$ differs substantially from that in pure $HoAl_2$. This might be due to some difference between the band structures of the two compounds; alternatively, it could be a local effect in the neighbourhood of the solute ions.

Let us now re-examine the theoretical basis for our *a priori* estimate of the exchange coefficient. One questionable feature of the model outlined in § 3.2 is the assumption that the variation of $\mathcal{J}_0$ across the RAl_2 series is associated solely with the coupling coefficient $\mathcal{A}(R)$. If we allow $f(\boldsymbol{r})$ to depend on the host medium, it will be convenient to recast equation (16) in the form

$$\mathcal{J}_0(R{:}R') = \mathcal{A}(R)\mathcal{A}(R')F(R') \tag{30}$$

where $F(R)$ stands for the sum $\Sigma_j f(\boldsymbol{r}_{ij})$ evaluated in pure RAl_2. It follows from equation (8) that

$$\mathcal{J}_0(R{:}R') = \{\mathcal{J}_0(R)\mathcal{J}_0(R')F(R')/F(R)\}^{1/2} \tag{31}$$

(cf equation (17)).

The additional free parameter $F(R')/F(R)$ allows us to reconcile any given values for the quantities $\mathcal{J}_0(R)$, $\mathcal{J}_0(R')$ and $\mathcal{J}_0(R{:}R')$. Explicitly,

$$F(R)/F(R') = \mathcal{J}_0(R)\mathcal{J}_0(R')/[\mathcal{J}_0(R{:}R')]^2 \tag{32}$$

and

$$\mathcal{A}(R)/\mathcal{A}(R') = \mathcal{J}_0(R{:}R')/\mathcal{J}_0(R'). \tag{33}$$

The experimentally determined weighted mean value of $\mathcal{J}_0(Ho{:}Gd)$, combined with the values of $\mathcal{J}_0(Gd)$ and $\mathcal{J}_0(Ho)$ given in §3.4, imply that $F(Ho)/F(Gd) = 2.1 \pm 0.4$ [1.0] and $\mathcal{A}(Ho)/\mathcal{A}(Gd) = 0.59 \pm 0.06$ [0.87 ± 0.06]; the figures in square brackets correspond to the original model in which F is constant across the series.

Another consequence of the model under discussion is that the simple reciprocity relationship (18) between $\mathcal{J}_0(R{:}R')$ and $\mathcal{J}_0(R'{:}R)$ is replaced by

$$\mathcal{J}_0(R'{:}R) = \{F(R)/F(R')\}\mathcal{J}_0(R{:}R') = \mathcal{J}_0(R)\mathcal{J}_0(R')/\mathcal{J}_0(R{:}R'). \tag{34}$$

This gives $\mathcal{J}_0(Gd{:}Ho)/k = (44 \pm 6)$ K. Setting $\langle J_z \rangle = (7.51 \pm 0.04)$ for $HoAl_2$ (II) we obtain $\alpha_{ex}/k = (80 \pm 10)$ K for Gd^{3+} in $HoAl_2$ at liquid helium temperatures in zero field. This may be compared with (54 ± 6) K and (37 ± 1) K, the values of α_{ex} derived from the '*a priori*' formula (17) and from the reciprocity relationship (18), respectively. A direct determination of the effective molecular field seen by Gd^{3+} in $HoAl_2$ would clearly be a useful test of the models under consideration.

The introduction of $F(R)$ as an adjustable parameter offers a formal solution for the problem of the effective exchange parameter, but provides a less satisfactory explanation for the variation of $\mathcal{J}_0(R)$ across the RAl_2 series. The rather rapid variation of both $F(R)$ and $\mathcal{A}(R)$ required by our data is a less plausible basis for the relatively slow variation of $\mathcal{J}_0(R)$ illustrated in figure 3 of I. Moreover, the simple physical explanation for the variation of the exchange constant in terms of the contraction of the radius of the 4f shell is now supplemented by another mechanism whose origin is far from clear. An alternative possibility is that the molecular field seen by an R ion in $R'Al_2$ is a localised effect associated with a virtual bound state. On this hypothesis there is no obvious connection between $\mathcal{J}_0(R{:}R')$ and the exchange coefficients for the terminal compounds. Detailed theoretical analysis will be required to ascertain whether or not the observed molecular

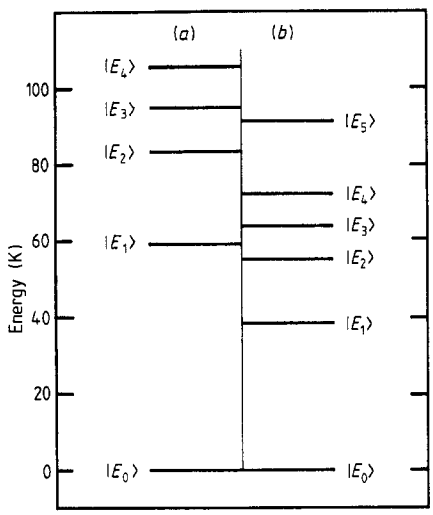

Figure 4. Calculated low-lying energy levels of Ho^{3+} in ferromagnetic $GdAl_2$ in zero applied field at low temperatures: (*a*) using the *a priori* exchange and crystal-field coefficients (top row of table 1); (*b*) using the coefficients derived from the NMR data (second row of table 1). See table 3 for details of the corresponding magnetic-dipole transitions.

field is in fact explicable in terms of a virtual bound state, but an order-of-magnitude estimate suggests that this hypothesis is at least a plausible one (Belorizky 1989).

Further measurements are clearly desirable in order to establish the systematics of exchange and crystal-field coefficients for dilute solute ions in $GdAl_2$ and in other RAl_2 hosts. In this context, we note that Ross *et al* (1983) have obtained unexpected results for the effective exchange coefficients for Pr^{3+} in $GdAl_2$ and in $NdAl_2$. Their value for $\mathcal{J}_0(\mathrm{Pr{:}Gd})$ is less than half that given by $\{\mathcal{J}_0(\mathrm{Pr})\mathcal{J}_0(\mathrm{Gd})\}^{1/2}$; that for $\mathcal{J}_0(\mathrm{Pr{:}Nd})$ nearly 20% *greater* than $\{\mathcal{J}_0(\mathrm{Pr})\mathcal{J}_0(\mathrm{Nd})\}^{1/2}$. However, both figures are based on *a priori* estimates of the crystal-field coefficients for Pr^{3+} in $GdAl_2$ and in $NdAl_2$; they are therefore open to question in view of the unexpected values of B_4 and B_6 obtained in present work. Berthier and Devine (1980b) also report effective molecular fields for Tb and Er in $GdAl_2$ which are significantly lower than those expected. Like Ross *et al* (1983), they assume that the crystal-field parameters for R in $GdAl_2$ are in the same as those for RAl_2; moreover, their 'expected' values of the molecular field are based on the implicit assumption that $\mathcal{J}_0(\mathrm{R{:}Gd}) = \mathcal{J}_0(\mathrm{Gd})$, i.e. that the exchange coefficient is independent of R.

We have already noted the desirability of measuring the effective molecular field seen by gadolinium in $HoAl_2$. The fact that Gd^{3+} is not subject to appreciable crystal-field anisotropy or quenching precludes the resonance techniques described in the present work; the effective field could however be obtained directly from a measurement of the exchange splitting by neutron inelastic scattering. Equally, the TPMF parameters for Ho^{3+} in $GdAl_2$ given in table 1 could usefully be checked by a neutron measurement of the low-lying energy levels. In figure 4 we show the two level schemes calculated from the *a priori* parameters and from the parameters derived from our NMR measurements. A neutron study of the Ho: $GdAl_2$ system would be beset by severe problems due to the enormous neutron absorption cross sections of the naturally occurring isotopes of gadolinium, and should ideally be carried out with a sample containing enriched ^{160}Gd. However, the differences between the two level schemes shown in figure 4 are probably large enough to be resolved by neutrons of sufficiently high energy to overcome the absorption problem in the natural isotopic mixture.

In table 3 we give the calculated frequencies for the strongly allowed magnetic-dipole

Table 3. Magnetic-dipole transitions from the ground state and from the first-excited state of Ho^{3+} in $GdAl_2$ in zero field. Only transitions with matrix elements exceeding 1 Bohr magneton are listed.

	A priori parameters[a]		Fitted parameters[b]	
Transition	Frequency (THz)	$\lvert\langle n\rvert\boldsymbol{\mu}\lvert m\rangle\rvert^2$ (μ_B^2)	Frequency (THz)	$\lvert\langle n\rvert\boldsymbol{\mu}\lvert m\rangle\rvert^2$ (μ_B^2)
$\lvert E_0\rangle \rightarrow \lvert E_1\rangle$	1.2 ± 0.1	14.6	0.80 ± 0.03	14.8
$\lvert E_0\rangle \rightarrow \lvert E_3\rangle$	1.9 ± 0.2	2.4	1.33 ± 0.05	1.8
$\lvert E_1\rangle \rightarrow \lvert E_2\rangle$	0.51 ± 0.05	29.5	0.35 ± 0.01	28.1
$\lvert E_1\rangle \rightarrow \lvert E_4\rangle$	1.0 ± 0.1	5.6	0.71 ± 0.02	4.5

[a] First row of table 1.
[b] Second row of table 1.

transitions from the ground and first-excited states of Ho^{3+} together with the appropriate squared matrix elements. Only the transitions from $|E_0\rangle$ can be excited at liquid helium temperatures, but the $|E_1\rangle \rightarrow |E_2\rangle$ transition should be observable at temperatures over 15 K if the 'fitted' parameter set is correct. The transition frequencies have been calculated using exchange fields appropriate to $T = 0$, but temperature-induced shifts will be unimportant up to at least 20 K. (The reduction in the molecular field is only 2% at 25 K if α_{ex} scales with the magnetisation: see du Tremolet de Lacheisserie (1988).)

5. Conclusions

NMR and FMR measurements on single crystals show that the three-parameter mean-field model provides an excellent description of the behviour Ho^{3+} in $GdAl_2$ at low temperatures. However, the experimentally determined crystal-field coefficients differ markedly from those for pure $HoAl_2$; moreover, the effective exchange coefficient between solute and host is not simply related to the exchange coefficients for the pure terminal compounds.

Possible explanations for the unexpected results just mentioned have been considered, but must remain tentative until the systematics of exchange and crystal-field interactions in dilute R: R′Al_2 alloys have been more firmly established. It is hoped that this paper will provide a stimulus for such investigations, in which neutron inelastic resonance measurements could play a decisive role.

Acknowledgments

We gratefully acknowledge the generous advice and assistance Dr D St P Bunbury with computing problems and of Dr P W Mitchell with non-linear least-squares fitting procedures. We are also indebted to Dr C Carboni for the design of the resonant cavity used for our NMR measurements and to Professor E Belorizky for illuminating comments. Our work was supported by a Research Grant from the Science and Engineering Research Council (SERC). DFM was supported by a SERC Research Studentship; Z-PH is supported by a Manchester University Research Scholarship.

Appendix. Equilibrium directions of the holmium and gadolinium moments in an applied field

When the field is applied in an arbitrary direction relative to the crystallographic axes, the gadolinium and holmium moments are not in general collinear with each other or with $\boldsymbol{B}_a$. In order to diagonalise $\mathcal{H}_{el}$ and so to estimate the angular dependence of the hyperfine splitting, we need to find how the magnitude and direction of $\boldsymbol{\alpha}$ (equation (3)) vary with the orientation of $\boldsymbol{B}_a$. By equations (4) and (15), $\boldsymbol{\alpha}_{ex}$ is parallel to the gadolinium spin $\langle\boldsymbol{\sigma}'\rangle$; moreover, the magnitude of $\boldsymbol{\alpha}_{ex}$ is constant since Gd^{3+} is not subject to crystal-field quenching. Our problem, therefore, reduces to finding the direction of $\langle\boldsymbol{\sigma}'\rangle$.

In what follows we assume that the gadolinium ions have negligible anisotropy. That being the case, $\langle\boldsymbol{\sigma}'\rangle$ will be parallel to the vector

$$\boldsymbol{\alpha}' = (g' - 1)\boldsymbol{X}' + g'\mu_B(\boldsymbol{B}_a + \boldsymbol{B}_{dip}) \tag{A.1}$$

where $\boldsymbol{X}'$, the exchange field seen by the Gd ions, is

$$\boldsymbol{X}' = \mathcal{A}(\mathrm{Gd}) \sum_j \mathcal{A}(\mathrm{R}_j) f(\boldsymbol{r}_{ij}) \langle\boldsymbol{\sigma}_j\rangle \tag{A.2}$$

(cf equations (3), (4) and (15)). Since, by hypothesis, those $\langle\boldsymbol{\sigma}_j\rangle$ belonging to Gd ions are collinear with $\boldsymbol{\alpha}'$, they cannot affect its direction. A similar consideration applies to the dipolar field, apart from the quite negligible contribution of the Ho ions to $\boldsymbol{B}_{dip}$. Thus, in order to find the *direction* of the Gd spins, we may replace $\boldsymbol{\alpha}'$ in equation (A.1) by the vector

$$\boldsymbol{D} = (g' - 1)\boldsymbol{X}'_{\mathrm{Ho}} + g'\mu_B\boldsymbol{B}_a \tag{A.3}$$

where

$$\boldsymbol{X}'_{\mathrm{Ho}} = \mathcal{A}(\mathrm{Gd})\mathcal{A}(\mathrm{Ho})\langle\boldsymbol{\sigma}\rangle \sum_j^{\mathrm{Ho}} f(\boldsymbol{r}_{ij}). \tag{A.4}$$

Here $\langle\boldsymbol{\sigma}\rangle = (g - 1)\langle\boldsymbol{J}\rangle$ is the Ho spin and the superscript (Ho) restricts the sum over j to those sites occupied by Ho ions. To an adequate approximation for the present purpose we may write, for 1% Ho in $GdAl_2$,

$$\sum_j^{\mathrm{Ho}} f(\boldsymbol{r}_{ij}) \simeq 0.01 \sum_j f(\boldsymbol{r}_{ij}). \tag{A.5}$$

Substituting (A.5) into (A.4) and using equation (16), we obtain

$$\boldsymbol{X}'_{\mathrm{Ho}} \simeq 0.01\mathcal{J}_o(\mathrm{Ho:Gd})\langle\boldsymbol{\sigma}\rangle \tag{A.6}$$

whence

$$\boldsymbol{D} \simeq 0.01\mathcal{J}_o(g - 1)\langle\boldsymbol{J}\rangle + g'\mu_B\boldsymbol{B}_a. \tag{A.7}$$

In this way we obtain the direction of $\boldsymbol{\alpha}_{ex}$ (which, as explained above, is parallel to $\boldsymbol{D}$) for any given values of $\langle\boldsymbol{J}\rangle$ and $\boldsymbol{B}_a$; the magnitude and direction of $\boldsymbol{\alpha}$ follow straightforwardly from equation (3). In practice, we use an iterative procedure starting with an initial guess of $\langle\boldsymbol{J}\rangle$ for each value of $\boldsymbol{B}_a$. Diagonalising $\mathcal{H}_{el}$ with the resulting value of $\boldsymbol{\alpha}$, we obtain the next approximation for $\langle\boldsymbol{J}\rangle$; the process is repeated until further iteration

gives negligible change. The final value of α is then used to compute the hyperfine parameters for the holmium ion.

References

Abell J S, Jones D W and Lee E W 1986 *J. Less-Common Met.* **115** 331–6
Abragam A and Bleaney B 1971 *Résonance paramagnétique Électronique des Ions de Transition* (Presses Universitaires de France)
Aleonard R, Morin P and Rouchy J 1988 *J. Physique Coll.* **49** C8 367–8
Bak P 1974 *J. Phys. C: Solid State Phys.* **7** 4097–103
Barash Y B and Barak J 1984 *J. Phys. F: Met. Phys.* **14** 1531–9
Barbara B and Berthier Y 1977 *Physica* B **86–88** 1385–7
Barbara B, Boucherle J X, Rossignol M F and Schweizer J 1977 *Physica* B **86–88** 83–4
Barbara B, Rossignol M F, Belorizky E and Levy P M 1983 *Solid State Commun.* **46** 669–72
Barbara B, Rossignol M F and Boucherle J X 1975 *Phys. Lett.* **55A** 321–2
Belorizky E 1989 private communication
Belorizky E and Berthier Y 1986 *J. Phys. F: Met. Phys.* **16** 637–50
Belorizky E, Berthier Y and Devine R A B 1984 *J. Magn. Magn. Mater.* **44** 313–28
Belorizky E, Fremy M A, Gavigan J P, Givord D and Li H S 1987 *J. Appl. Phys.* **61** 3971–3
Belorizky E, Gavigan J P, Givord D and Li H S 1988a *Europhys. Lett.* **5** 349–54
—— 1988b *J. Physique Coll.* **49** C8 4112
Berthier Y and Devine R A B 1980a *Phys. Rev.* B **21** 3844–50
—— 1980b *J. Magn. Magn. Mater.* **15–18** 703–5
Bleaney B 1972 *Magnetic Properties of Rare Earth Metals* ed. R J Elliott (New York: Plenum) pp 383–420
Bowden G J, Cadogan J M, Doolan K R, Martinson P J and Pope J M 1982 *J. Phys. F: Met. Phys.* **12** 363–76
Bowden G J, Cadogan J M, Fairbairn W M and Griffin D A 1983 *J. Phys. F: Met. Phys.* **13** 191–205
Bunbury D St P, Carboni C and McCausland M A H 1989 *J. Phys: Cond. Matter* **1** 1309–27
Campbell I A 1972 *J. Phys. F: Met. Phys.* **2** L47–50
Carboni C, Cone R L, Han Z-P and McCausland 1988 *J. Physique Coll.* **49** C8 843–4
Carboni C, Mackenzie I S and McCausland 1989 *Hyperfine Interact.* **51** 1139–44
Crosswhite H M, Crosswhite H, Edelstein N and Rajnak K 1977 *J. Chem. Phys.* **67** 3002–10
Dormann E, Dressel U, Kropp H and Buschow K H W 1984 *J. Magn. Magn. Mater.* **45** 207–18
Dressel U and Dormann E 1988 *J. Physique Coll.* **49** C8 455–6
Dressel U, Meister U, Dormann E and Buschow K H W 1988 *J. Magn. Magn. Mater.* **74** 91–100
Dumelow T, Reidi P C, Abell J S and Prakash O 1988 *J. Phys. F: Met. Phys.* **18** 307–22
Dunlap B D, Nowik I and Levy P M 1973 *Phys. Rev.* B **7** 4232–41
Eyers A, Alke A, Leson A, Kohake D and Purwins H-G 1982 *J. Phys. C: Solid State Phys.* **15** 2459–69
Fekete D, Grayevskey A, Kaplan N and Walker E 1975 *Solid State Commun.* **17** 573–6
Frauenheim Th, Matz W and Feller G 1979 *Solid State Commun.* **29** 805–9
de Gennes P G 1962 *J. Phys. Radiat.* **23** 510–21
Haberstroh R A, Moran T I and Penselin S 1972 *Z. Phys.* **252** 421–7
Harris I R, Mansey and Raynor G V 1965 *J. Less-Commun. Met.* **9** 270–80
Holden T M, Buyers W J L and Purwins H-G 1984 *J. Phys. F: Met. Phys.* **14** 2701–18
Kohake D, Leson A, Purwins H-G and Furrer A 1982 *Solid State Commun.* **43** 965–8
Kropp H, Dormann E, Grayevsky A and Kaplan N 1983 *J. Phys. F: Met. Phys.* **13** 207–14
Leson A, Schelp W, Drewes W and Purwins H-G 1986 *J. Magn. Magn. Mater.* **54–57** 473–4
Levy P M 1969 *Solid State Commun.* **7** 1813–8
McCausland M A H and Mackenzie I S 1979 *Adv. Phys.* **28** 305–456
McMorrow D F, Carboni C, McCausland M A H and Abell J S 1986 *J. Magn. Magn. Mater.* **54–57** 485–6
Morin P and Schmitt O 1988 *J. Physique Coll.* **49** C8 321–5
Prakash O, Bunbury D St P and McCausland M A H 1984 *Z. Phys.* B **58** 39–48
Purwins H-G, Walker E, Barbara B, Rossignol M F and Bak P 1974 *J. Phys. C: Solid State Phys.* **7** 3573–81
Purwins H-G, Walker E, Barbara B, Rossignol M F and Furrer A 1976 *J. Phys. C: Solid State Phys.* **9** 1025–30
Rajnak K and Krupke W F 1967 *J. Chem. Phys.* **46** 3532–42
Rhyne J J and Koon N C 1983 *J. Magn. Magn. Mater.* **31–34** 608–10

Ross J W, Prakash O and McCausland M A H 1983 *J. Phys. F: Met. Phys.* **13** L95–8
Rushbrooke G S and Wood P J 1958 *Mol. Phys.* **1** 257–83
Schelp W, Drewes W, Purwins H-G and Eckold G 1985 *J. Magn. Magn. Mater.* **50** 147–52
Schelp W, Leson A, Drewes W, Purwins H-G and Grimm H 1983 *Z. Phys.* B **51** 41–7
Schelp W, Drewes W, Leson A and Purwins H-G 1986 *J. Phys. Chem. Solids* **47** 855–61
Schmitt D, Morin P and Pierre J 1977 *Phys. Rev.* B **15** 1698–1705
Smart J S 1966 *Effective Field Theories in Magnetism* (London: Saunders)
Taylor K N R 1971 *Adv. Phys.* **20** 551–660
Teale R W, Oner T and Han Z-P 1989 *J. Phys: Condens. Matter* **1** 3841–7
du Tremolet de Lacheisserie E 1988 *J. Magn. Magn. Mater.* **73** 289–98
Waind P R, Mackenzie I S and McCausland M A H 1983 *J. Phys. F: Met. Phys.* **13** 1041–56
Zipper E, Kaczmarska K, Kwapulinska E and Pichet J 1984 *J. Magn. Magn. Mater.* **40** 259–64